

# **ANALYZING WIND-DRIVEN RAIN ON A BUILDING FACADE USING THE LASER PRECIPITATION MONITOR (LPM)**

Ayyapan Kumaraperumal<sup>†</sup>, Chris H. Sanders, Paul H. Baker, Graham H. Galbraith, and Don McGlinchey

*Centre for Research on Indoor Climate and Health,  
School of Engineering, Science & Design, Glasgow Caledonian University,  
Glasgow, United Kingdom*

## **ABSTRACT**

This paper is concerned with a building situated in the west of Scotland which faces severe weather conditions with high wind speeds and driving rain occurring frequently. This results in extensive damage to the building fabric, and affects the internal climate which leads to a serious issue in building construction. In this study, a three-dimensional numerical model of airflow around the building is investigated. This investigation is part of ongoing research on wind-driven rain which has established the importance of moisture stresses, wind flow and rain impacts on a commercial building. The full scale experimental facility which includes anemometers, rain gauge, driving rain gauges and sensors is described. To supplement this, a sophisticated laser precipitation monitor (disdrometer) was installed, which collects rain data every 1-minute. This provides accurate measurement of drop size and speed of the falling raindrops which plays an important role in wind-driven rain studies.

Comparisons with numerical simulations and experimental data were predicted. Results shows that the average predominantly wind direction for the sample test period is from south-west (223<sup>o</sup> from north) and the driving rain during this period is 86.8 mm for the west facing façade and 193.4 mm for the south facade. From the computational fluid dynamics (CFD) simulations, it is predicted that the change in velocity profile along the laser strip is due to the test building and the disdrometer head itself, which ultimately affects the driving rain calculations.

## **KEYWORDS**

Wind flow, Wind-driven rain (WDR), Computational fluid dynamics (CFD), Indoor air quality, Disdrometer

## **INTRODUCTION**

Rapid changes in the UK construction industry make a huge impact on commercial buildings which range from small shops to huge business stores. Protecting these buildings from the severe external climate is a challenging task. Among this, wind-driven rain (WDR) which is the combination of wind and rain is the most important factor while considering external climate. Continuous exposure of building facades to high levels of driving rain keeps the level of moisture contents high. This leads to moisture penetration inside the building which can make mould growth likely and ultimately affects the indoor air quality. Appropriate design and construction techniques are needed to prevent rain water penetrating building facades. Proper design of drainage channels for run off and roof overhangs can limit the rain

---

<sup>†</sup> Corresponding Author: Tel: + 44 141 3313688, Fax: + 44 141 3313690

E-mail address: aku1@gcal.ac.uk

water penetration but some is unavoidable.

Recent studies by some researchers (Sanders 2004, Blocken et al. 2007 and Kumaraperumal et al. 2006) on WDR shows the importance of WDR in various practical aspects like heat, air and moisture [HAM] transfer, effects on indoor air quality due to the moisture presence in the indoor facades and many other examples related to the broad topic of buildings and environmental physics. Apart from full-scale experimental and numerical simulations, a semi-empirical relationship is frequently used in estimating WDR in building facades. This is the basis of the British Standard Code of practice BSI (BS8104 1992), for assessing the exposure of a wall to wind-driven rain, the only available standard method for estimation driving rain quantities in the UK. On the basis of BS8104, a draft CEN (CEN 1997) standard is in preparation based on the work done by Sanders (Sanders 1996) which requires hourly values of rainfall, wind speed and wind direction. In this paper, experimental results and CFD predictions for wind flow and rain drop impact have been analyzed for one commercial building.

### GENERAL DESCRIPTION OF THE EXPERIMENT

The experiment is conducted on a commercial building, Building Research Establishment (BRE) Scotland which is situated in East Kilbride, in an exposed area near to the centre of the city and exposed to the most common direction from where the wind blows the south-west. The full-scale experiment has been carried out at the topmost section of the building as shown in the figure 1. The dimensions of the main building are 40.46m (length), 12m (width) and 10.25m (height). Acquisition of weather data started from May 2005, and from January 2006 more sensors and instruments were mounted on the site. Figure 1 shows the list of mounted instruments on the BRE building. From the 12.25m height mounted anemometer the reference wind velocity and direction are measured and used for the computer simulation purposes.

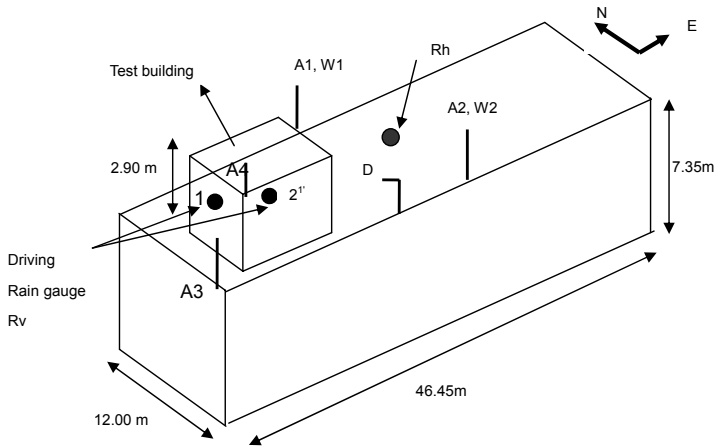


Figure 1. 3-D view of BRE test building (figure not in scale)

From figure 1, A1, V1 (Anemometer, Wind vane) is 12.25m height from the ground (reference height), A2, V2 (Anemometer, Wind vane) is 8.60m, A3 (Anemometer) is 8.60m, A4 (Anemometer) is 10.55m,

D-Disdrometer is mounted 2.5m near to the south façade of building, Rv - wind-driven rain, Rh- rain gauge measuring horizontal rainfall and S is a sunshine sensor (measure global horizontal sunshine state). These sensors record wind speed, wind direction, rainfall intensity and wind driven rain intensity. Moreover temperature and relative humidity sensors were mounted on the interior and exterior of the building component for the calculations of moisture contents.

### **Laser Precipitation monitor (LPM) or Disdrometer**

Normal rain gauges (like tipping bucket rain gauge) provide the total height of water fallen during a particular period of time. The response from the rain gauge is sufficient to utilize the information for climatology or general meteorological purposes. For studying the falling velocities and the size distribution of the raindrops, a relatively new instrument called a 'Disdrometer' or laser precipitation monitor (LPM), shown in Figure 2 can be used. The LPM is capable of distinguishing between liquid droplets and solid hydrometers and recording particle speed and size i.e. classification of hydrometeors according to size and terminal velocity.

### **Working principle of LPM**

The LPM consists of a laser diode and optics which produces a parallel light-beam of 0.75mm thickness with a detection area of 20 × 228 mm. The principle of measurement is the occultation of the parallel beam of infrared light by falling raindrops. When the precipitation particle falls through the light beam the received signal is reduced. The amplitude of the reduction is related to the size of the particles, and the duration of the reduction is related to the fall speed (Thies Clima 2003). The type of precipitation is determined from the statistical distribution of the diameter and velocity of all particles. The disdrometer was acquired to get more information of rain falling on the wall façade. Initially it was intended to mount the disdrometer vertically on the wall, so that actual distribution of rain particle hitting on the wall could be obtained. But for the safety reasons of the instrument and for the people working around, we have mounted disdrometer on the railing at the edge of the roof of the building (facing south-west direction) which is also approximately 2m away from the west building test façade.

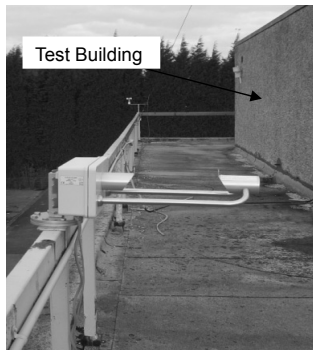


Figure 2. Laser precipitation monitor

All data are given in synchronously recorded 1-minute intervals, leading to a maximum of 1440 measurements per day. For every 1 minute the precipitation monitor provide output of 443 items of data, including the intensity of precipitation, number of measured particles, number of particles with different

speed, etc. The impact of rainfall on wall facades is dependant on the terminal velocity of the fall. Several equations have been published that describe the terminal velocity of fall as a function of the drop diameter. In this work we were comparing the results based on two important empirical laws which have been studied experimentally (Gunn and Kinzer 1949) and (Best 1950) (equation 1 and 2). For the comparison of the data, two rainy days during December 2006 have been examined using the LPM.

$$V(a) = 9.40 \left[ 1 - \exp(-1.57 \times d^{1.15}) \right] \quad (\text{Gunn and Kinzer 1949}) \quad (1)$$

$$V(a) = 9.55 \left\{ 1 - \exp[-1.15(d)^{1.147}] \right\} \quad (\text{Best 1950}) \quad (2)$$

Where  $V(a)$  is the terminal velocity of falling rain drop, in m/s, and  $d$  is the drop diameter in mm.

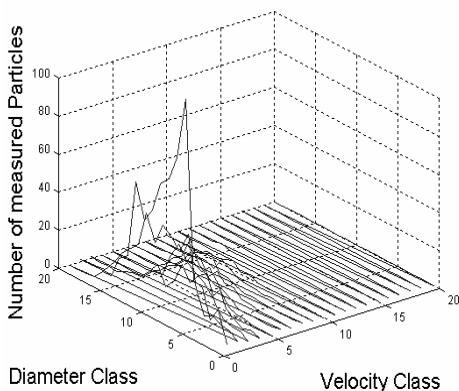


Figure 3: Raindrop size distribution

Analyzing the large amount of output data produced each minute by the disdrometer is a difficult task. Initially there were some difficulties in reading the data, but these were overcome by a Matlab program developed to read and analyze the data.

Figure 3 shows that, for a particular minute the LPM output data consists of the number of particles,  $n_i$ , per diameter class,  $d_i$ , and per velocity class,  $V_i$ . Diameters in 20 categories ranges in size from 0.125mm to 7.0mm, and the range of the fall speed of drops range from 0.2 m/s to 10 m/s, the velocity  $V_i$  is distributed into 20 size intervals. In this particular case, the total number of particle measured per minute is 1647 and the maximum number of drops recorded is 59, in diameter class  $2.5 < d < 3$  and velocity class  $3.4 < V < 4.2$ ; as well as these, 633 numbers of particles have classified as other than hydrometeors.

Figure 4 compares the LPM data with equations 1) and 2); it can be seen that the largest measured raindrop data by disdrometer is 3.5mm and the velocity ranges from 7.4 to 8.2 m/s and the result varies widely compared to the standard equations. The reason may be the mounting position of the disdrometer and the obstruction caused by the test building is causing turbulence which slows the fall rate of the drops.

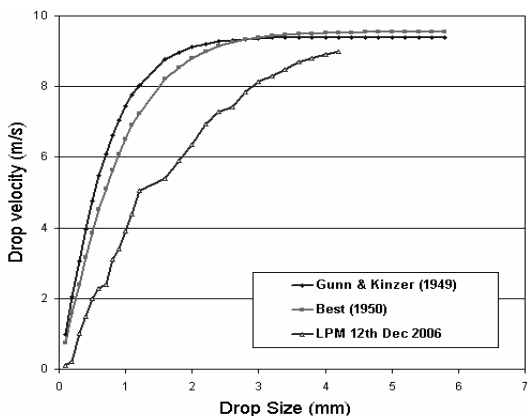


Figure 4. Measured terminal speed of drop as a function of drop size

### Reference rain gauge

For the purpose of accuracy of the results it is reasonable to compare the disdrometer data to a traditional rain gauge. The rain gauge information is obtained from the tipping bucket rain gauge which is mounted on the roof of the building without any nearby obstructions. Detailed measurements of wind speed and direction during periods of heavy rain were carried out with special attention to the magnitude of the higher value of wind speed and wind direction during that period. The average wind speed during for November and December 2006 is 3.10 m/s and driving rain recorded during this period for west and south facades are 86.8 mm and 193.4 mm respectively. The hourly rainfall measured for the period of two months from both the rain gauge (502.6 mm) and laser precipitation (327.56 mm) shows slight differences in the measured data of rain gauge and disdrometer.

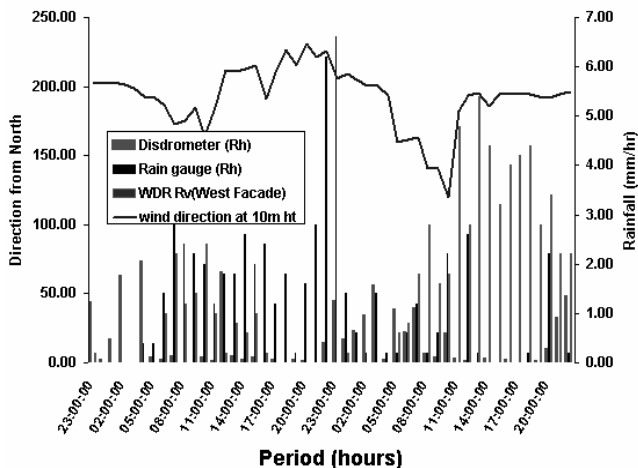


Figure 5. Hourly recorded data on 12th and 13th December 2006

But by considering the data for two rainy days during December, it can be noted that the difference between rain gauge and disdrometer data is much greater (Figure 5). The hourly rainfall measured from both the rain gauge and laser precipitation monitor vary slightly. The reason may be the rain gauge is mounted on the horizontal ground without any nearby obstacles while the disdrometer is mounted on railing of the BRE building and may face some obstacles of rain during the north-west wind flow. So it is necessary to understand the effect of wind flow on the mounted disdrometer.

## NUMERICAL SIMULATION

In order to assess the influence of wind on the mounted disdrometer, 3-D wind flow simulations around the disdrometer and building were computed. The air flow field is modelled in three dimensions using FLUENT (Fluent 2006) (version 6.3), solving the Reynolds-averaged Navier-Stokes and continuity equations numerically to obtain the steady-state velocity field. Closure is achieved with the aid of the realizable  $k-\epsilon$  turbulence model, where  $k$  is the turbulent kinetic energy and  $\epsilon$  is the turbulent kinetic energy dissipation. The flow field around the disdrometer and building were computed at different wind speed and wind incidence angles of  $180^\circ$  and  $270^\circ$  from North. For the  $180^\circ$  wind direction case, the computational domain extended to  $15H$  in the upwind direction,  $15H$  downwind of the BRE building, and  $15H$  m to the sides and  $16H$  from the ground. The computational domain is relatively large as compared to the proposed domain in the literature (Frank et al. 2004). The reason for considering the large domain is to incorporate the rain falling from certain height and to cover the entire building.

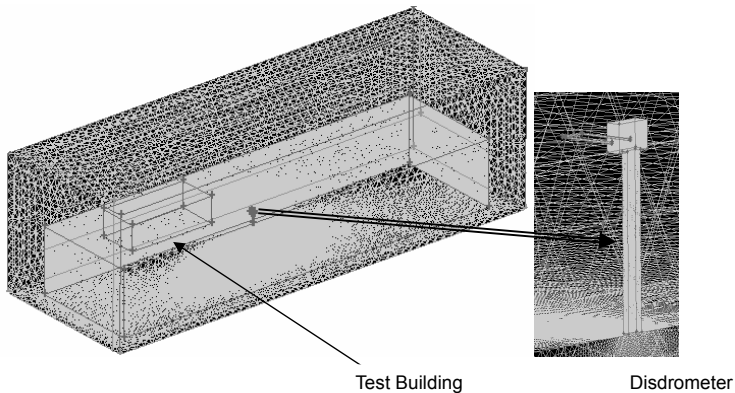


Figure 6. CFD Mesh for BRE building

The unstructured mesh, containing 2.2 million nodes, was constructed so that the density of nodes was highest near the disdrometer (figure 6) and ground. The velocity was calculated using the log-law equation. For atmospheric boundary layer (ABL), the inlet logarithmic velocity profile has 10m/s wind speed, frictional velocity is 0.872m/s and the aerodynamic roughness length is 0.1 m, in order to fit the measure velocity profile. Figure 7 shows the 2-D top view of BRE building and the position of mounted disdrometer on the railing of the building. Horizontal wind velocity profiles across the disdrometer have been calculated numerically (Figure 8). From Fig.8, it is clearly seen that the velocity acceleration on the windward side and deceleration (recirculation zones) on the downwind side i.e. behind the

disdrometer head.

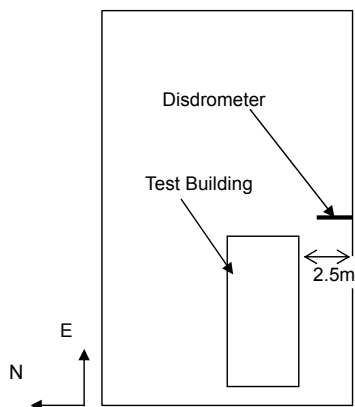


Figure 7. 2-D BRE building (Top View)

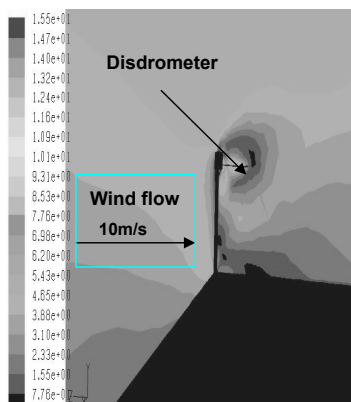


Figure 8. Velocity Counter plot for 10m/s wind speed using Realizable  $k-\epsilon$  model

From figure 9, we can predict the effects of nearby obstacles (like test building or the disdrometer head itself) to the disdrometer which can affect the wind profile along the axis of emitted laser on the disdrometer. By plotting the velocity vector, it can be seen that for 0 degree wind direction and 10 m/s wind speed, there is a non uniform velocity wind profile due to the presence of the building. Hence from the above observation it is predicted that the mounting of the instrument plays a vital role in the WDR measurements.

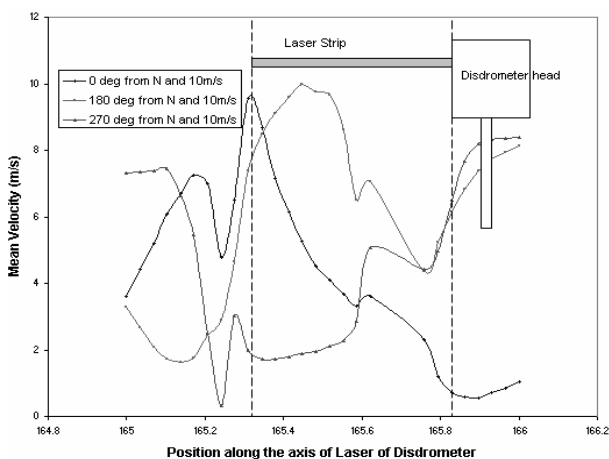


Figure 9. Velocity vector near disdrometer

## CONCLUDING REMARKS

- It is seen that disdrometer is capable of measuring individual particle and records less rain compared to the reference rain gauge.
- Investigations have been performed with preliminary numerical simulations to explain the wind flow profile around the disdrometer.
- The Fluent<sup>®</sup> program calculates the distribution of mean velocity across the building and the disdrometer. The result indicates high velocity near the windward corner of the building facade. But the real concern is the flow simulation around the disdrometer. It is noted that, for high wind velocity (10m/s), the head of the instrument may cause eddies which may displace the rain particles out of the laser strip.
- We continue our investigation by increasing the sample data and analyzing with further numerical simulation of raindrop trajectories and its effects on this wind field. More scenarios with different rainfall intensities, wind speed and wind directions will be considered.

## REFERENCES

1. C. Sanders (2004) "Comparison of the 'British Standard' and 'French' methods for estimating driving rain impacts on walls", IEA Annex 41 meeting Glasgow, Report A41-T3-UK-04-2.
2. B. Blocken, S. Roels and J. Carmeliet (2007) "A combined CFD-HAM approach for wind-driven rain on building facades", Journal of wind engineering and industrial aerodynamics. Industrial Aerodynamics, doi:10.1016/j.jweia.2006.12.001.
3. A. Kumaraperumal, P.H Baker, C. Sanders, G.H Galbraith and McLean R.C (2006) "Prediction of fabric moisture contents in historic building using CFD and heat, air and moisture transfer modelling compared with full-scale measurements", 7th UK conference on wind engineering. Glasgow, UK.
4. British Standard Institution (1992) "BS8104: Code of practice for assessing exposure of walls to wind-driven rain", London, United Kingdom.
5. CEN (1997) "Hygrothermal performance of buildings- Climatic data- part 3: Calculation of a driving rain index for vertical surfaces from hourly wind and rain data", Draft prEN 13013-3.
6. C. Sanders (1996) "Environmental Condition, International Energy Agency", IEA Annex 24, Final Report, Volume 2, Task2, ISBN 90-75741-03-0.
7. Thies Clima (2003) "laser precipitation monitor instruction for use", 5.4110.00.200. Website <http://www.thiesclima.com/disdrometer.htm>
8. R. Gunn and G.D. Kinzer (1949) "The terminal velocity of fall for water droplets in stagnant air", Journal of Meteorology 6: 243-248.
9. A. Best (1950) "The size distribution of raindrops", Quarterly journal of the royal meteorological society 76: 16-36.
10. J. Frank, C. Hirsch, A.G. Jensen, S.D. Miles, M. Schatzmann, P.S. Westbury, J.A. Wisse and N.G. Wright (5-7 May 2004) "Proceedings of the International Conference on Urban Wind Engineering and Building Aerodynamics, COST Action C14, Impact of Wind and Storm on City Life Built Environment. von Karman Institute, Sint-Genesius-Rode, Belgium.
11. Fluent Inc., 2006, Fluent 6 user's guide.